Controlled Lagrangian Particle Tracking Error Under Biased Flow Prediction

Klementyna Szwaykowska and Fumin Zhang

Abstract— **In this paper we model the controlled Lagrangian particle tracking (CLPT) error for marine vehicles moving in an ocean flow field, with guidance from ocean models. We linearize the error about the nominal modeled trajectory of the system and derive an exact expression for the linearized error in the case of constant modeled ocean flow. We show that this simple error model can be used to estimate error in predicted positions of autonomous vehicles, using data from a field deployment of autonomous underwater gliders in Long Bay, SC, in winter 2012.**

I. Introduction

In recent years, autonomous underwater vehicles (AUVs) have emerged as an exciting technology in the field of oceanographic research. Traditional sensor platforms commonly used in oceanography include moored arrays, ships, and drifting surface platforms. AUVs have lower operating costs than the scientific vessels used for research, and are easier to deploy and recover than moored platforms. They also have the advantage of active mobility, so that, unlike drifting or moored platforms, they can be sent to probe different locations of interest within the changing ocean environment. This makes them particularly useful in ocean monitoring missions that require mobility and long-duration deployments (see for example [1]). Multiple AUVs may be deployed together for improved coverage of the survey area and improved data collection, as in [2], [3]. An overview of the development of unmanned underwater vehicles is given in [4].

During extended deployments, using path planning and navigation algorithms can significantly improve the value of collected data. In existing literature, there are numerous examples of path-planning algorithms for vehicles in flow. One possible approach includes dynamic programming methods, as in [5], which find a globally optimal path. More commonly, faster heuristic algorithms are used. Garau *et al* use an A* algorithm to generate min-time paths for AUVs in spatially varying, time-static flows [6], [7]. Pêtrès *at al* use a Fast Marching (FM)-based algorithm for efficient path planning in a static flow field [8]; their method is generalized by Soulignac *at al*, to strong [9] and time-varying flows [10]. An alternative approach, not related to dynamic programming, is to use genetic algorithms, as in [11], or case-based path planning [12].

All of these path planning algorithms rely on accurate prediction of the AUV's trajectory in the given flow field over time. This is difficult to guarantee in practice, since the AUVs' motion is strongly affected by ambient flow. Flow velocity can be obtained from ocean general-circulation models (OGCMs); however, ocean models often include errors due to missing physics, limited resolution, and errors in the model forcing terms and boundary conditions. In a typical setup, a large-scale ocean model is used to drive the regional model used for flow prediction in a glider deployment. This results in complex, multi-scale errors in the driven model, an effect known as the uncertainty cascade [13], [14]. The error in the Eulerian flow field in turn causes errors in the predicted AUV trajectories.

Our approach is controlled Lagrangian particle tracking (CLPT). This is a variation of Lagrangian particle tracking, a well-established approach in oceanography which is used to study motions of freely advected particles in ocean flows [15]–[19]. CLPT models the motions of vehicles with controlled velocity inputs. The vehicle is modeled as a particle whose velocity is the sum of ambient flow and through-water velocity. To analyze the error in vehicle position prediction, we consider a pair of concurrent experiments, in which a "real" vehicle and its "virtual" counterpart are initialized at a given position and propagated forward. We then compare the trajectories of the two vehicles and measure the separation between them over time. This separation is termed the CLPT error. In this paper, we expand earlier results in [20], [21], where we derived bounds on CLPT error growth for particles operating under perfect flow cancellation with constant flow modeling error. In this paper, we derive an approximate formula for growth of error in the predicted position of a feedback-controlled particle moving in a flow field under guidance from a flow model, with arbitrary control strategy. We give an analytical result for error growth in the case of spatially constant flow with constant model bias. This simple case serves as an illustrative example of the effect of ocean modeling error on error in predicted particle positions. We demonstrate that constant model bias is a significant factor in the growth of position prediction error by comparing theoretical predictions of CLPT error growth with the error in predicted position of underwater gliders in a field deployment in Long Bay, SC, in winter of 2012.

The rest of this paper is organized as follows: the problem set-up and general equation for CLPT error growth are described in section II. In this section we also describe a particular example of first-order particle dynamics and a station-keeping controller. The position prediction error growth in the simple case with constant ambient flow is derived in section III. Simulation results are shown in section IV, and concluding remarks are given in section V.

{klimka,fumin}@gatech.edu, Georgia Institute of Techonology, Atlanta, GA 30318

II. Problem Set-Up

Controlled Lagrangian particle tracking is used to model the motions of vehicles (i.e., controlled particles) with controlled velocity inputs in ocean flow fields. Let $\mathbf{x}$ denote the state of the vehicle, defined over domain $\mathcal{D}$. In general, the net velocity of the vehicle is a function of the vehicle state, control input u, and the ambient water velocity $\mathbf{F}$:

$$\frac{\mathrm{d}\mathbf{x}(t)}{\mathrm{d}t} = g(\mathbf{x}(t), \mathbf{F}(\mathbf{x}, t), u(\mathbf{x}, \mathbf{F}, t)). \tag{1}$$

The functional form of g depends on the internal vehicle dynamics, the hydrodynamic coupling between vehicle and ambient flow, and on the ambient flow velocity. Errors can enter the model in a number of places, causing the modeled vehicle position to diverge from the true position observed in the field; we classify them broadly as errors in the modeled vehicle dynamics (including errors in the modeled coupling between ambient flow and vehicle motion) and errors in the modeled flow dynamics. In the case of slow-moving vehicles moving in complex flow environments with a reasonable model of the vehicle motion, the error in modeled position is dominated by the latter error source; that is, error in the modeled flow conditions. We therefore focus on this error source in the current work.

To simplify the error computations, we assume a simple first-order vehicle model as the fiducial model for total vehicle motion. The net vehicle velocity is given by a simple sum of the vehicle's through-water velocity and the ambient flow. Let $\mathbf{x} \in \mathcal{D}$ denote the state of the vehicle in configuration space $\mathcal{D}$; let $\mathbf{v} : \mathcal{D} \times \mathbb{R} \to T\mathcal{D}$ be the through-water velocity, and let $\mathbf{F}_R : \mathcal{D} \times \mathbb{R} \to T\mathcal{D}$ be the velocity of the ambeint flow, expressed in state-space coordinates (here $T\mathcal{D}$ denotes the tangent bundle of $\mathcal{D}$):

$$\frac{\mathrm{d}\mathbf{x}(t)}{\mathrm{d}t} = \mathbf{v}(\mathbf{x}, t) + \mathbf{F}_R(\mathbf{x}, t). \tag{2}$$

The position of the vehicle can be predicted using numerical integration of (2), with $\mathbf{F}_R$, the real flow velocity, replaced by its modeled value, $\mathbf{F}_M$. Let $\mathbf{z}(t)$ denote the modeled vehicle position.

Let $\mathbf{e}_s$ denote the state prediction error, defined as the offset between true and modeled vehicle states:

$$\mathbf{e}_s \triangleq \mathbf{x} - \mathbf{z}. \tag{3}$$

The time evolution of $\mathbf{e}_s$ is described by

$$\begin{aligned} \dot{\mathbf{e}}_s &= \mathbf{F}_R(\mathbf{x}, t) + \mathbf{v}(\mathbf{x}, t) - \mathbf{F}_M(\mathbf{z}, t) - \mathbf{v}(\mathbf{z}, t) \\ &= \mathbf{f}(\mathbf{x}, t) + \mathbf{F}_M(\mathbf{x}, t) - \mathbf{F}_M(\mathbf{z}, t) + \mathbf{v}(\mathbf{x}, t) - \mathbf{v}(\mathbf{z}, t) \end{aligned} \tag{4}$$

where $\mathbf{f}(\zeta, t) \triangleq \mathbf{F}_R(\zeta, t) - \mathbf{F}_M(\zeta, t)$ is the error in modeled flow velocity. We find a first-order approximation of the error growth in predicted vehicle position using a Taylor expansion of the error growth equation about the simulated vehicle trajectory.

For convenience, let $\mathbf{V}$ denote the net velocity of the vehicle under modeled flow:

$$\mathbf{V}(\zeta, t) \triangleq \mathbf{F}_M(\zeta, t) + \mathbf{v}(\zeta, t). \tag{5}$$

Furthermore, let $\mathbf{z}(t)$ denote the simulated vehicle position at time t, with $\mathbf{z}(t_0) = \mathbf{x}(t_0)$. Since $\mathbf{z}(t)$ is a known function of time, we can apply a change of coordinates $\zeta \mapsto \zeta - \mathbf{z}(t)$ and define:

$$\bar{\mathbf{f}}(\mathbf{e}_s, t) \triangleq \mathbf{f}(\mathbf{z}(t) + \mathbf{e}_s, t) \tag{6}$$

$$\bar{\mathbf{V}}(\mathbf{e}_s, t) \triangleq \mathbf{V}(\mathbf{z}(t) + \mathbf{e}_s, t).. \tag{7}$$

Then (4) can be written as

$$\dot{\mathbf{e}}_s = \bar{\mathbf{f}}(\mathbf{e}_s, t) + \bar{\mathbf{V}}(\mathbf{e}_s, t) - \bar{\mathbf{V}}(0, t). \tag{8}$$

Taking the first-order Taylor expansion of (8) about the simulated vehicle trajectory gives:

$$\dot{\mathbf{e}}_s \approx \mathrm{D}\bar{\mathbf{V}}(0, t)\mathbf{e}_s + \bar{\mathbf{f}}(\mathbf{e}_s, t) \tag{9}$$

Equation (9) can be interpreted as a time-varying linear system with a state-dependent disturbance $\bar{\mathbf{f}}$. In general, we can say very little about the behavior of $\mathbf{e}_s$ over time. In this paper, we consider a special simple case of this equation, where $\mathrm{D}\bar{\mathbf{V}}$ has a simple time variation.

A. Constant-speed particle model

We consider a simple constant-speed kinematic particle model for the motions of underwater vehicles. The selection of this model is justified by our field experience with underwater gliders; these slow-moving autonomous vehicles behave like particles over sufficiently long time scales (hours-days).

We choose state variables $\mathbf{x} = [\mathrm{x}_1, \mathrm{x}_2]^T \in \mathcal{D} = \mathbb{R}^2$ and $\mathbf{z} = [\mathrm{z}_1, \mathrm{z}_2]^T \in \mathcal{D} = \mathbb{R}^2$ represent the horizontal positions of the real and simulated vehicles, respectively. The constant though-water vehicle speed is given by $s \in \mathbb{R}_+$, and is assumed to be the same for both the real and simulated vehicles. The real and simulated vehicle positions are given by

$$\dot{\mathbf{x}} = s\mathbf{n}(u(t, \mathbf{x})) + \mathbf{F}_R(t, \mathbf{x}), \tag{10}$$

$$\dot{\mathbf{z}} = s\mathbf{n}(u(t, \mathbf{z})) + \mathbf{F}_M(t, \mathbf{z}), \tag{11}$$

where $\mathbf{n}$ is a unit vector in the direction u, the commanded heading angle.

B. Station-keeping controller

In this paper, we consider a station-keeping mission, in which the vehicles' desired direction of motion is always toward a fixed goal $\mathbf{g}$. Near the goal position, the vehicle therefore behaves as a "virtual mooring". This control algorithm was utilized by our group in the field. Without loss of generality, we choose the coordinate system so that $\mathbf{g} = 0$.

To perform station-keeping control with guidance from ocean models, the heading u is chosen to cancel the modeled flow velocity in the direction normal to the desired motion. Let $\mathbf{T}$ be the unit vector from the vehicle position to the goal $\mathbf{g}$, and let $\mathbf{N}$ be normal to $\mathbf{T}$. For $\mathbf{g} = 0$, $\mathbf{T}(\mathbf{x}) = -\frac{\mathbf{x}}{\|\mathbf{x}\|}$ and $\mathbf{N} = \frac{J\mathbf{x}}{\|\mathbf{x}\|}$, where J is the 90° rotation matrix. Let $\mathbf{v} = s\mathbf{n}(u)$ denote the vehicle through-water velocity. Under the flow-canceling controller, u is chosen so that net motion is

along $\mathbf{T}$. Assuming $\| \mathbf{F}_M \| < s$ everywhere (so that flow cancellation is always possible), this means that:

$$\mathbf{v}^T\mathbf{N} = -\mathbf{F}_M^T\mathbf{N}. \tag{12}$$

To satisfy (12), we must have $u(\mathbf{x}) = \tan^{-1}\frac{\mathbf{x}_2}{\mathbf{x}_1} + \pi - \sin^{-1}\frac{\mathbf{F}_M^T\mathbf{N}}{s}$ (see Fig. 1).

Since $\| \mathbf{v} \|^2 = s^2 = (\mathbf{v}^T\mathbf{T})^2 + (\mathbf{v}^T\mathbf{N})^2 = (\mathbf{v}^T\mathbf{T})^2 + (\mathbf{F}_M^T\mathbf{N})^2$, where the last equality follows from (12), and since we require $\mathbf{v}^T\mathbf{T} > 0$ (that is, the vehicle moves toward the goal), the through-water velocity component along $\mathbf{T}$ is given by $\mathbf{v}^T\mathbf{T} = \sqrt{s^2 - (\mathbf{F}_M^T\mathbf{N})^2}$.

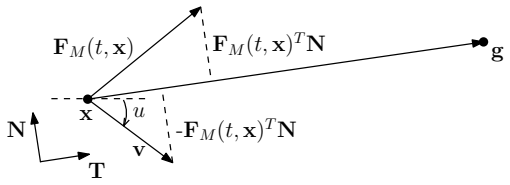

Fig. 1. Schematic of flow-canceling station-keeping controller.

Using the notation defined in (5), under flow-canceling station-keeping control described in this section, we have:

$$\mathbf{V}(\mathbf{x}) = \left((\mathbf{F}_M^T\mathbf{T}) - \sqrt{s^2 + (\mathbf{F}_M^T\mathbf{N})^2} \right) \mathbf{T}, \tag{13}$$

for $\mathbf{F}_M(\mathbf{x})^T\mathbf{N}(\mathbf{x}) \leq s$. We can now derive the error in position prediction for a specified flow field and flow modeling error for a vehicle moving with dynamics described by the constant-speed particle model and controller given by the station-keeping flow-canceling control. Our goal is to quantify the forward propagation from error in the ocean model flow to error in predicted position.

III. Error in the predicted vehicle positions: a simple case

In this section we consider position prediction error in a simple case, where the ambient flow is constant, and satisfies the condition $\| \mathbf{F}_M \| \leq s$. We consider an underwater vehicle with dynamics are given by the constant-speed kinematic particle model with flow-canceling station-keeping control.

In this case it is very easy to compute the position of the simulated vehicle $\mathbf{z}(t)$; the vehicle travels in a straight line to the goal with constant speed $\mathbf{F}_M^T\mathbf{T} + [s^2 - (\mathbf{F}_M^T\mathbf{N})^2]^{1/2}$. Note that since the simulated vehicle travels in a straight line, $\mathbf{T} = \frac{\mathbf{z}(t)}{\| \mathbf{z}(t) \|}$ and $\mathbf{N} = J\mathbf{T}$ are constant vectors. For notational convenience, we define the following constants, $\alpha, \beta \in \mathbb{R}$:

$$\alpha = \frac{\mathbf{F}_M^T J\mathbf{T}}{\sqrt{s^2 - (\mathbf{F}_M^T J\mathbf{T})^2}} \tag{14}$$

$$\beta = \mathbf{F}_M^T\mathbf{T} + \sqrt{s^2 - (\mathbf{F}_M^T J\mathbf{T})^2}. \tag{15}$$

Note that β is the simulated vehicle's total speed toward the origin. We also define the constant matrix

$$A = (\mathbf{T}\mathbf{F}_M^T + \alpha\mathbf{T}\mathbf{F}_M^T J + \beta I)(I - \mathbf{T}\mathbf{T}^T). \tag{16}$$

The following lemma will be used in computing the growth of position prediction error:

Lemma 3.1: Given A defined by (16), $A^i = \beta^{i-1}A$.

Proof: Let $M = (I - \mathbf{T}\mathbf{T}^T)$. For A defined as in (16), we have $A^2 = [\mathbf{T}\mathbf{F}_M^T M + \alpha\mathbf{T}\mathbf{F}_M^T JM - \beta M]^2$. Expanding this expression and using the fact that $M\mathbf{T} = 0$ and $M^2 = (I - \mathbf{T}\mathbf{T}^T)^2 = M$ gives

$$A^2 = \beta(\mathbf{T}\mathbf{F}_M^T + \alpha\mathbf{T}\mathbf{F}_M J - \beta I)M = \beta A. \tag{17}$$

Lemma 3.1 follows by applying (17) i times. ∎

The growth of position prediction error in the constant flow case is summarized in the following proposition:

Proposition 3.1: Given real and simulated vehicles with dynamics described by (10) and (11), respectively, with flow-canceling station-keeping control, and constant model flow $\mathbf{F}_M$ such that $\| \mathbf{F}_M \| \leq s$, the error in predicted position of the controlled particle grows as:

$$\begin{aligned}\mathbf{e}_s(t) = &\left(I - \frac{t}{\| \mathbf{z}_0 \|} A \right) \mathbf{e}_s(0) \\ &+ \left(I - \frac{t}{\| \mathbf{z}_0 \|} A \right) \int_0^t \left(I + \frac{\eta}{\| \mathbf{z}_0 \| - \beta\eta} A \right) \mathbf{f}(\mathbf{z}, t) \mathrm{d}\eta\end{aligned} \tag{18}$$

for $t \in [0, \| \mathbf{z}_0 \| / \beta)$.

Proof: By (9), the evolution of the error is given to first order by

$$\dot{\mathbf{e}}_s = D\bar{\mathbf{V}}(0)\mathbf{e}_s + \bar{\mathbf{f}}(\mathbf{e}_s), \tag{19}$$

where, (using (13) for $\mathbf{V}$),

$$\begin{aligned}D\bar{\mathbf{V}}(0) = &\left(\mathbf{T}(\mathbf{z})\mathbf{F}_M^T - \frac{\mathbf{F}_M^T J\mathbf{T}(\mathbf{z})}{\sqrt{s^2 - (\mathbf{F}_M^T J\mathbf{T}(\mathbf{z}))^2}} \mathbf{T}(\mathbf{z})\mathbf{F}_M^T J \right. \\ &\left. + \left(\mathbf{F}_M^T\mathbf{T}(\mathbf{z}) + \sqrt{s^2 - (\mathbf{F}_M^T J\mathbf{T}(\mathbf{z}))^2} \right) I \right) D\mathbf{T}(\mathbf{z}).\end{aligned} \tag{20}$$

Using α, β in (20) and the fact that $D\mathbf{T}(\mathbf{z}) = -D\frac{\mathbf{z}}{\| \mathbf{z} \|} = -\frac{I - \mathbf{T}(\mathbf{z})\mathbf{T}(\mathbf{z})^T}{\| \mathbf{z} \|}$, and plugging into (19), we have that the first-order approximation of the error in predicted vehicle position increases as

$$\begin{aligned}\dot{\mathbf{e}}_s &= \frac{-(\mathbf{T}\mathbf{F}_M^T + \alpha\mathbf{T}\mathbf{F}_M^T J - \beta I)(I - \mathbf{T}\mathbf{T}^T)}{\| \mathbf{z}(t) \|} \mathbf{e}_s + \mathbf{f} \\ &= \frac{-1}{\| \mathbf{z}(t) \|} A\mathbf{e}_s + \mathbf{f},\end{aligned} \tag{21}$$

where A is defined as in (16). We can solve (21) exactly as:

$$\begin{aligned}\mathbf{e}_s(t) = &\, e^{-\int_0^t \frac{1}{\| \mathbf{z}(\tau) \|} A \mathrm{d}\tau} \mathbf{e}_s(0) \\ &+ e^{-\int_0^t \frac{1}{\| \mathbf{z}(\tau) \|} A \mathrm{d}\tau} \int_0^t e^{\int_0^\eta \frac{1}{\| \mathbf{z}(\tau) \|} A \mathrm{d}\tau} \mathbf{f} \mathrm{d}\eta.\end{aligned} \tag{22}$$

Let $\mathbf{z}(0) = \mathbf{z}_0$ be the initial position of the simulated vehicle. The vehicle will travel in a straight line toward the origin with speed β, so that $\mathbf{z}(t) = \left(1 - \frac{\beta t}{\| \mathbf{z}_0 \|} \right) \mathbf{z}_0$, and $\| \mathbf{z}(t) \| = \| \mathbf{z}_0 \| - \beta t$ for $t < \frac{\beta}{\| \mathbf{z}_0 \|}$. Then

$$-\int_0^t \frac{1}{\| \mathbf{z}(\tau) \|} A \mathrm{d}\tau = \frac{1}{\beta} \log \left(\frac{\| \mathbf{z}_0 \| - \beta t}{\| \mathbf{z}_0 \|} \right) A. \tag{23}$$

The exponential of this is given by the series definition:

$$e^{\frac{1}{\beta}\log\left(\frac{\|\mathbf{z}_0\|-\beta t}{\|\mathbf{z}_0\|}\right)A} = \sum_{i=0}^{\infty} \frac{\left(\log\frac{\|\mathbf{z}_0\|-\beta t}{\beta\|\mathbf{z}_0\|}\right)^i A^i}{i!}. \quad (24)$$

Using Lemma 3.1 and simplifying the algebraic expression we get:

$$e^{-\int_0^t \frac{1}{\|\mathbf{z}(\tau)\|}A\mathrm{d}\tau} = e^{\frac{1}{\beta}\log\left(\frac{\|\mathbf{z}_0\|-\beta t}{\|\mathbf{z}_0\|}\right)A} = I - \frac{t}{\|\mathbf{z}_0\|}A. \quad (25)$$

Similarly,

$$e^{\int_0^t \frac{1}{\|\mathbf{z}(\tau)\|}A\mathrm{d}\tau} = I + \frac{t}{\|\mathbf{z}_0\|-\beta t}A. \quad (26)$$

Using (25) and (26) in (22) proves the Proposition. ■

Assuming that the real and simulated vehicles are initialized to the same position, so that $\mathbf{e}_s(0) = 0$, we can consider the growth in position prediction error due to error $\mathbf{f}$ in the ocean model flow prediction. For constant $\mathbf{f}$, corresponding to a constant model bias, (18) evaluates to:

$$\mathbf{e}_s(t) = \left[t\left(I - \frac{1}{\beta}A\right) - \frac{\|\mathbf{z}_0\|-\beta t}{\beta^2}\log\frac{\|\mathbf{z}_0\|-\beta t}{\|\mathbf{z}_0\|}A\right]\mathbf{f}. \quad (27)$$

It is straightforward to show that the error along the direction of travel, $\mathbf{e}_s(t)^T\mathbf{T}$, is given by $tf_{\mathbf{T}} - 1/\beta(t + \frac{\|\mathbf{z}_0\|-\beta t}{\beta}\log\frac{\|\mathbf{z}_0\|-\beta t}{\|\mathbf{z}_0\|})(F_{M,\mathbf{N}} - \alpha F_{M,\mathbf{T}})f_{\mathbf{N}}$, where $f_{\mathbf{T}}$ and $f_{\mathbf{N}}$ denote the components of $\mathbf{f}$ along $\mathbf{T}$ and $\mathbf{N}$, respectively, and similarly, $F_{M,\mathbf{T}}$ and $F_{M,\mathbf{N}}$ denote the components of $\mathbf{F}_M$. As there is no feedback control along the vehicle's direction of travel, the error growth in this direction is dominated by the linear term in t. Normal to the direction of travel, the error $\mathbf{e}_s(t)^T\mathbf{N}$ is given by $-\frac{\|\mathbf{z}_0\|-\beta t}{\beta}\log\frac{\|\mathbf{z}_0\|-\beta t}{\|\mathbf{z}_0\|}$. This error initially grows as the vehicle is pushed off-course by the bias flow, and is later reduced as the vehicle steers toward the station-keeping goal. Thus, in the case of constant flow and constant model bias, we can find an analytical simple solution for the linearized error growth for a vehicle under station-keeping control.

IV. Simulation and Experimental Results

We present several simulations as well as field experiment data to show that, in the case of spatially uniform bias flow in the predicted ocean flow field, the theoretical first-order estimate position-prediction error gives a good approximation of error growth in predicted vehicle positions.

The vehicles used are Slocum electric gliders, which are slow-moving, buoyancy-propelled AUVs, with effective through-water speed of about 0.24 m/s. The gliders use onboard waypoint-following algorithms with dead-reckoning while underwater, and surface periodically (with a period of 3-4 hours) to communicate with an on-shore controller. Simulations are run using the Glider Environment Networked Information System (GENIOS), a Matlab-based software package for glider simulation and control based on the Glider Coordinated Control System (GCCS) developed at Princeton in 2006. GENIOS includes a planning module (*gplan*) which generates waypoints to specify glider trajectories as well as a simulator module (*gsim*). *Gsim* uses predicted flow data from ocean models together with a three-dimensional glider model, and emulates the glider's on-board control algorithms to generate realistic glider trajectories. A more detailed description of GCCS can be found in [22], [23].

Our field experiment was run in Long Bay, SC, in winter of 2012. Two gliders were used in the deployment to monitor ocean conditions over an extended period between January and April 2012, to study mechanisms that lead to the formation of persistent wintertime phytoplankton blooms in this area. Both gliders used the station-keeping controller described in section II-B; one glider performed a virtual-mooring mission at the edge of the gulf stream, while the second glider switched between two station-keeping goal positions which marked the endpoints of a cross-shore transect, achieving a transect-following behavior. GENIOS was used to generate waypoint lists for both gliders; waypoints were followed using the glider's on-board proprietary navigation software. We focus our simulations on the transect-following glider. In all figures in this section, the blue line next to the glider trajectories shows the relative position of the transect. The station-keeping goal is the middle "dot" along the transect. We ran two simulations, described below.

Simulation I

Two gliders are simulated using *gsim* with flow-canceling station-keeping control, under a constant-flow ocean model with $\mathbf{F}_M = [0.15,\ 0.03]^T$ m/s. The "real" glider moves in a field $\mathbf{F}_R = \mathbf{F}_M + \mathbf{f}$, where $\mathbf{f} = [-0.0764 - 0.0083]$ m/s is a constant bias flow. We predict the error in glider position using (27) and compare this with the true offset between the "real" and "virtual" glider trajectories (see Figure 2). The theoretical error prediction is based on glider dynamics described in (10)-(11) and is given by (27). So long as the vehicle is far from the goal and $\mathbf{f}$ is not too strong, the theoretical prediction of position prediction error based on the linearization in (9) gives a good approximation of the true error value. A sample trajectory is shown in Figure 2. This helps to justify our use of first-order error dynamics in the simple flow case.

Simulation II

In the second simulation, we use the same set-up as in Simulation I. This time, however, the flow data F_M comes from a tidal database generated from a series of simulations run by B. Blanton, using the Advanced Circulation (ADCIRC) ocean model [24]. We use this simulation to verify that the first-order error model gives a reasonable approximation of the position prediction error under more complex flow conditions. In this case, Lemma 3.1 no longer holds, since matrix A is no longer constant. In this case, we therefore integrate (9) numerically using Euler's method to find theoretical position prediction error values over time. Figure 3 shows the simulation results. The error computed using (9) closely matches the true error between the "virtual" glider simulated with ADCIRC flow only, and the "real" glider, which operates under an additional bias flow.

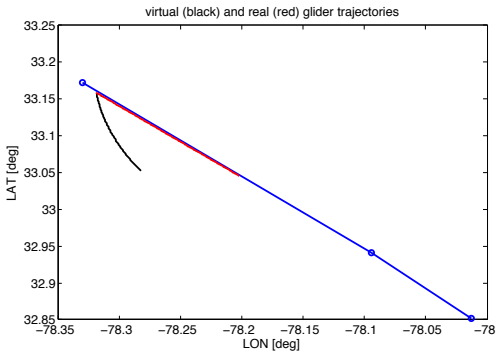

(a)

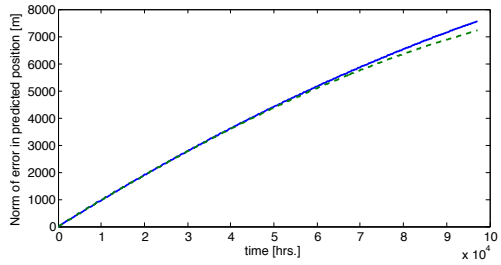

(b)

Fig. 2. Subfigure 2(a): trajectories of real and two station-keeping gliders in constant flow (positions are given in latitude-longitude coordinates; the glider's goal position corresponds to a point near Long Bay, SC). Subfigure 2(b): norm of the error in predicted glider trajectory. Solid lines show observed error, dashed lines show theoretical error prediction.

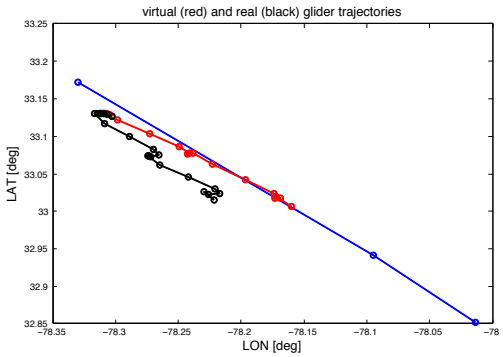

(a)

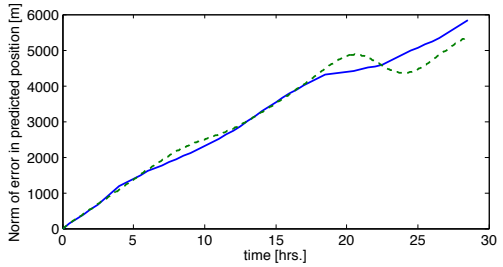

(b)

Fig. 3. Subfigure 3(a): trajectories of real and virtual station-keeping gliders in tidal flow predicted by ADCIRC (positions are given in latitude-longitude coordinates; the glider's goal position corresponds to a point near Long Bay, SC). The real glider experiences a constant bias flow not captured by the ADCIRC model. Subfigure 3(b): norm of error in the predicted glider trajectory. Solid lines show observed error, dashed lines show theoretical error prediction.

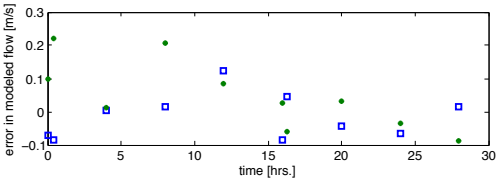

Fig. 4. Error in ADCIRC prediction of Eastward (squares) and Northward (stars) depth-averaged flow values over each glider dive period, in m/sec. Glider on-board depth-averaged flow measurements are used as ground truth.

Field Experiment Results

As in Simulation II, the virtual glider is simulated in GCCS, with flow data from the ADCIRC tidal database. The real glider position is obtained from GPS measurements of glider surfacing positions for the transect-following glider over a 28-hour time period starting on Mar. 19, 2012 at 1:55 PM. The error $\mathbf{f}$ in modeled flow over this period is shown in Figure 4. It is clear that $\mathbf{f}$ does not represent a constant flow bias in this case. We computed the theoretical error in predicted position twice, first using constant model bias $\mathbf{f} = [-0.0764 - 0.0083]$ m/s (the mean bias flow observed over the period of the simulation). Second, to test the predictive capabilities of the linear error model, we computed the theoretical error value using a prediction of $\mathbf{f}$ values, obtained from harmonic analysis of the observed flow error for 7 days prior to Mar. 19th. The dominant harmonic components in error flow were used to forecast flow error over the 28-hour period of the simulation. The results are shown in Fig. 5.

The theoretical error computation based on linearized error dynamics with forecast $\mathbf{f}$ gives a less accurate estimate of the glider position prediction error than the theoretical error computed with constant $\mathbf{f}$. The root mean square (RMS) value of the difference between theoretical and observed error in predicted glider position is $1.3 \cdot 10^3$ in the case of forecast $\mathbf{f}$ and $7.6 \cdot 10^2$ in the case of constant $\mathbf{f}$. This reflects the fact that past values of $\mathbf{f}$ give a very poor estimate of future observed values. This result could perhaps be improved is a longer history of error flow values were available. In both cases, there are also contributions to error in the predicted glider position that are not taken into account by the linearized error model, including nontrivial glider dynamics and unknown coupling between flow and glider motions.

V. Conclusion

In this paper, we use a linearization of error dynamics about the predicted vehicle trajectory to model growth of error in predicted vehicle position over time, and show, using simulations, that the linearized error gives a good approximation of the true position prediction error value for a station-keeping autonomous vehicle operating far from the desired station-keeping position. We have applied this result to compute expected error in the position predicted for a transect-following glider during a field deployment in Long

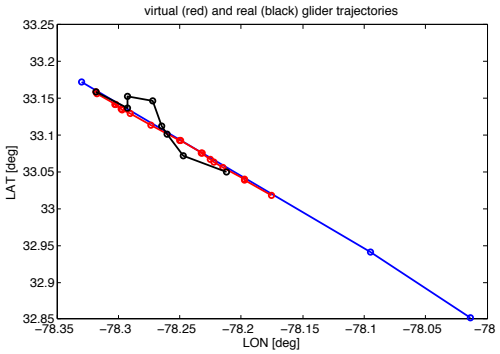

(a)

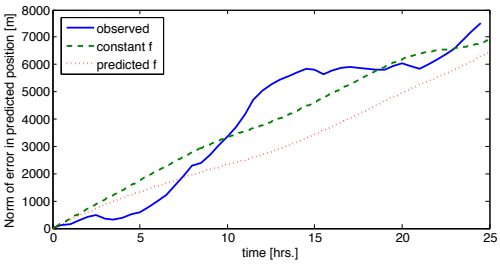

(b)

Fig. 5. Subfigure 5(a): trajectories of real and virtual station-keeping gliders from a field experiment in Long Bay, SC, in winter 2012. The virtual glider position is simulated using flow from the ADCIRC tidal database. Subfigure 5(b): norm of the error in predicted glider trajectory assuming constant bias error (dashed line) and predicted periodic error (dotted line) in modeled flow. Solid lines show observed error at glider surfacing times.

Bay, where the glider was using station-keeping control and was far from its station-keeping goal.

In our future work, we will extend the approach used in this paper to estimate error in glider position prediction under more complex, time-varying flows, and in the case where the model error in predicted flow is modeled as a stochastic process. These cases more accurately reflect the conditions observed in the field; however, analytical results are much more difficult to obtain. Our goal is to define bounds on the position prediction error and error growth rate in this case.

Acknowledgement

The research work is supported by ONR grants N00014-09-1-1074 and N00014-10-10712 (YIP), and NSF grants ECCS-0841195 (CAREER), CNS-0931576, and OCE-1032285. The authors want to thank Dr. Catherine Edwards of the Skidaway Institute of Oceanography for comments and discussions regarding glider operations during the Long Bay experiment.

References

[1] R. N. Smith, Y. Chao, P. P. Li, D. A. Caron, B. H. Jones, and G. S. Sukhatme, "Planning and implementing trajectories for autonomous underwater vehicles to track evolving ocean processes based on predictions from a regional ocean model," *The International Journal of Robotics Research*, vol. 29, pp. 1475–1497, Aug. 2010.

[2] P. Bhatta, E. Fiorelli, F. Lekien, N. E. Leonard, D. A. Paley, F. Zhang, R. Bachmayer, D. M. Fratantoni, R. E. Davis, and R. J. Sepulchre, "Coordination of an underwater glider fleet for adaptive sampling," in *Proceedings of the International Workshop on Underwater Robotics*, no. August, pp. 61–69, 2005.

[3] N. E. Leonard, D. A. Paley, R. E. Davis, D. M. Fratantoni, F. Lekien, and F. Zhang, "Coordinated control of an underwater glider fleet in an adaptive ocean sampling field experiment in Monterey Bay," *Journal of Field Robotics*, vol. 27, pp. 718–740, Nov. 2010.

[4] J. Yuh and M. West, "Underwater robotics," *Advanced Robotics*, vol. 15, no. 5, pp. 609–639, 2001.

[5] D. R. Thompson, S. Chien, M. Arrott, A. Balasuriya, Y. Chao, P. P. Li, M. Meisinger, S. Petillo, and O. Schofield, "Mission planning in a dynamic ocean Sensorweb," in *ICAPS SPARK*, vol. 91109, 2009.

[6] B. Garau, A. Alvarez, and G. Oliver, "Path planning of autonomous underwater vehicles in current fields with complex spatial variability: an A* approach," in *Proceedings of the 2005 IEEE International Conference on Robotics and Automation*, pp. 194–198, IEEE, 2005.

[7] B. Garau, M. Bonet, A. Alvarez, and S. Ruiz, "Path planning for autonomous underwater vehicles in realistic oceanic current fields: application to gliders in the western Mediterranean Sea," *Journal of Maritime Research*, vol. 6, no. 2, pp. 5–22, 2009.

[8] C. Pêtrès, Y. Pailhas, P. Patrón, Y. Petillot, J. Evans, and D. Lane, "Path planning for autonomous underwater vehicles," *IEEE Transactions on Robotics*, vol. 23, pp. 331–341, Apr. 2007.

[9] M. Soulignac, P. Taillibert, and M. Rueher, "Adapting the wavefront expansion in presence of strong currents," in *2008 IEEE International Conference on Robotics and Automation*, vol. 2008, pp. 1352–1358, IEEE, May 2008.

[10] M. Soulignac, P. Taillibert, and M. Rueher, "Time-minimal path planning in dynamic current fields," in *2009 IEEE International Conference on Robotics and Automation*, pp. 2473–2479, IEEE, May 2009.

[11] A. Alvarez, A. Caiti, and R. Onken, "Evolutionary path planning for autonomous underwater vehicles in a variable ocean," *IEEE Journal of Oceanic Engineering*, vol. 29, no. 2, pp. 418–429, 2004.

[12] C. Vasudevan and K. Ganesan, "Case-based path planning for autonomous underwater vehicles," *Autonomous Robots*, vol. 3, no. 2-3, pp. 79–89, 1996.

[13] E. Ferreira-Coelho and M. Rixen, "Maritime rapid environmental assessment new trends in operational oceanography," *Journal of Marine Systems*, vol. 69, pp. 1–2, Jan. 2008.

[14] M. Rixen, E. Ferreira-Coelho, and R. Signell, "Surface drift prediction in the Adriatic Sea using hyper-ensemble statistics on atmospheric, ocean and wave models: uncertainties and probability distribution areas," *Journal of Marine Systems*, vol. 69, pp. 86–98, Jan. 2008.

[15] F. B. Smith, "Conditioned particle motion in a homogeneous turbulent field," *Atmospheric Environment*, vol. 2, no. 5, pp. 491–508, 1968.

[16] H. van Dop, F. T. M. Nieuwstadt, and J. C. R. Hunt, "Random walk models for particle displacements in inhomogeneous unsteady turbulent flows," *Physics of Fluids*, vol. 28, no. 6, pp. 1639–1653, 1985.

[17] D. J. Thomson, "A random walk model of dispersion in turbulent flows and its application to dispersion in a valley," *Quarterly Journal of the Royal Meteorological Society*, vol. 112, pp. 511–530, Apr. 1986.

[18] A. Griffa, "Applications of stochastic particle models to oceanographic problems," in *Stochastic Modeling in Physical Oceanography* (R. J. Adler, P. Müller, and B. Rozovskii, eds.), pp. 113–140, Boston: Birkhäuser, 1996.

[19] A. C. Haza, L. I. Piterbarg, P. Martin, T. M. Özgökmen, and A. Griffa, "A Lagrangian subgridscale model for particle transport improvement and application in the Adriatic Sea using the Navy Coastal Ocean Model," *Ocean Modelling*, vol. 17, pp. 68–91, Jan. 2007.

[20] K. Szwaykowska and F. Zhang, "A lower bound for controlled Lagrangian particle tracking error," in *49th IEEE Conference on Decision and Control (CDC)*, pp. 4353–4358, Dec. 2010.

[21] K. Szwaykowska and F. Zhang, "A lower bound on navigation error for marine robots guided by ocean circulation models," in *2011 IEEE/RSJ International Conference on Intelligent Robots and Systems*, pp. 3583–3588, IEEE, Sept. 2011.

[22] D. A. Paley, *Cooperative control of collective motion for ocean sampling with autonomous vehicles*. Phd thesis, Princeton University, 2007.

[23] D. A. Paley, F. Zhang, and N. E. Leonard, "Cooperative control for ocean sampling: the Glider Coordinated Control System," *IEEE Transactions on Control Systems Technology*, vol. 16, pp. 735–744, July 2008.

[24] B. O. Blanton, "Barotropic tides in the South Atlantic Bight," *Journal of Geophysical Research*, vol. 109, no. C12, 2004.